Electromagnetic properties of chloroprene rubber after long-term ultraviolet ageing, oil immersion and thermal degradation

R. Sela[1], D. Bychanok[*2,3], Y. Padrez[2], D. Adamchuk[4], V. Ksenevich[4], N. Naveh[1], P. Kuzhir[2,3]**

[1] Polymers and Plastics Engineering Dept., Shenkar College of Engineering and Design, Ramat Gan 5252626, Israel

[2] Research Institute for Nuclear Problems Belarusian State University, Bobruiskaya str. 11, Minsk, 220030, Belarus

[3] Tomsk State University, 36 Lenin Prospekt, Tomsk 634050, Russian Federation

[4] Belarusian State University, Bobruiskaya str. 7, Minsk, 220030, Belarus

E-mail: * dzmitrybychanok@ya.ru, ** naumn@shenkar.ac.il

December 2018

Abstract.

The electromagnetic properties of chloroprene rubber after long-term ultraviolet ageing, oil immersion and thermal degradation were experimentally investigated in the frequency range from 1 kHz up to 1 THz. Ageing was shown in terms of mechanical degradation and the change in the complex dielectric permittivity. Within the whole investigated frequency range decrease of dielectric permittivity was observed after thermal treatment combined with oil immersion in comparison with chloroprene rubber stored under normal conditions. In contrast, thermal and ultraviolet ageing without immersion leads to increase of rubbers dielectric permittivity in all investigated frequency ranges. A non-invasive express method of degradation detection is proposed and proofed.

PACS numbers: 77.84.Jd, 42.25.Bs, 78.67.Wj, 78.67.Bf

Keywords: chloroprene rubber, long-term ultraviolet ageing, thermal degradation, dielectric spectroscopy

Submitted to: *Mater. Res. Express*

1. Introduction

Chloroprene rubber (CR) is one of the most important synthetic rubber resins widely used in industry. Its excellent characteristics such as weather and ozone resistance, good resistance to open fire, adhesion to fabrics and metals, fuel resistance make it a requisite source material for the mass production of mechanical rubber goods. Useful properties of CR may be effectively extended by using them in composite materials, and many recent investigations have proven CR as an effective dielectric matrix in composites production [1–3]. Rubber products in practical use are being exposed to environmental conditions during their service life. The rubber molecules are degraded by oxygen (O_2), ozone (O_3), heat, UV radiation, etc. The chemical degradation mechanism is free radical chain reaction [4] which proceeds through either chain scission or further crosslinking of the rubber molecules and hence to the ageing thus leading to loss of the original mechanical/physical properties. Natural rubber and butyl rubber usually respond by chain scission and turn sticky and soft, while nitrile rubber, chloroprene and SBR harden and become brittle because of crosslinking. In some cases, new functional groups are formed, which propagate the ageing process. Physical degradation also takes place, for instance when rubber is exposed to oil, grease or solvents. A proper choice of these should minimize the damage, nevertheless with time the combined effects of chemical and physical ageing lead to property change. Most rubber resins include carbon-carbon double bonds which act as crosslinking sites during processing, however some of them remain after crosslinking and are responsible for the accelerated ageing process of rubber, compared to plastics [4]. These chemical bonds are also responsible for the sensitivity to ozone, oxygen and halogens, thus limiting the shelf life and the working life of elastomeric goods.

Until now most investigations have focused on mechanical properties change with ageing, either static or relaxation and creep [5, 6] and chemical analysis of the rubber to identify new functional groups, a change in crosslink density or changes in specific gravity. There are only several works devoted to dielectric characteristics of CR as well as their change during degradation [2, 3, 7]. While non-destructive testing (NDT) of metals is well developed and certain NDT techniques, such as ultrasonic testing, are available also for defect detection in plastics and **rubber [8]**, further evaluation by NDT is not, especially for analysis of chemical degradation, viscoelastic effects such as relaxation or creep, and physical effects such as swelling due to solvents or fuel, a weakness of certain rubber compositions.

Dielectric spectroscopy provides a powerful tool for the design and production of materials with controlled mechanical properties and electromagnetic response. Particularly, the electromagnetic properties of important engineering and industrial materials are intensively investigated in the last decade [9–11]. Many investigations are devoted to development of materials with enhanced electromagnetic shielding performance [12–15]. The chlorinated polyethylene based polymer nanocomposites and the effect of the

thermal-air ageing treatment on their mechanical and electrical properties were considered in [16].

In the present manuscript we propose to apply conventional dielectric spectroscopy methods for detection of degradation in chloroprene rubber. In this work we focus on the ultra-broadband experimental characterization of electromagnetic (EM) properties of neat chloroprene rubber as is and after its long-term ultraviolet ageing, oil immersion and thermal treatment. The data include field ageing and laboratory ageing according to standards, that is, both long and short exposures to the ageing conditions. Since short UV exposure is usually not effective, short-term tests included oven ageing and exposure to oil. Detailed analysis of experimental data shows the possibility to use electromagnetic radiation for effective, quick and non-invasive testing of material degradation.

This paper is organized as follows: after the introduction (first section), the second section describes materials used and methods of their electromagnetic properties characterization. The third section presents the broadband experimental data of measured dielectric permittivity of samples under study. The presented frequency spectra of are analyzed, discussed and compared with investigations made by other research groups. The experimental results related to the electromagnetic response of the investigated materials in the microwave range (26-37 GHz) are examined more precisely in section 4. In this part of the manuscript, we also propose an express and non-invasive method of degradation discernment. The last section of the manuscript is devoted to the discussion of the presented results and summarizes the most important issues to the further practical usage of the materials studied.

2. Materials and methods

2.1. Materials

In present work the properties of five types of materials were studied: A) the neat CR, B) the CR aged under UV radiation, C) CR immersed with oil, D) CR thermally aged and E) CR thermally aged in combination with oil immersion.

The production and vulcanization ingredients of neat CR samples A-series was done by a laboratory size open two roll mixing mill. **The CR compound comprises Neoprene WHV (54 wt%), FEF carbon black (20 wt%), and a chlorinated plasticizer (16 wt%) as main components, and includes antioxidant and antiozonant [17]. The curing agent is 2-imidazolidinethione (ETU), a sulfur-based accelerator.** The neat CR samples **(A-series)** were used for production of the other samples series according to the following procedures of lab degradation.

B-series: UV ageing during 254 days according to ASTM G-154 using an ATLAS UV ageing chamber with UVA 340 nm fluorescent radiometric calibrated lamps.

C-series: Exposure to IRM 903 oil for 168 hours.

D-series: Thermal ageing in air for 72hr at 100°C.

E-series: Thermal ageing in oil according to ASTM D-471. "Dumbbell" and cylindrical disk samples were immersed in IRM 903 oil for 35 days at 100°C.

2.2. Methods

At the end of the exposure periods the mechanical properties of obtained samples were investigated using standard procedures. The samples were tested according to ASTM D-2240 for hardness. Tensile strength and elongation were tested according to ASTM D-412. Other standard rubber properties were established as per ASTM D-2000 and the methods shown in Table 1.

The electromagnetic properties were investigated at the room temperature using conventional broadband dielectric spectroscopy methods. Because the materials under study were non-magnetic, their EM characteristics are fully defined by complex dielectric permittivity, which frequency dependencies were investigated in three bands: low frequency (1 kHz - 2 MHz), microwave (26-37 GHz) and terahertz (0.2-1.0 THz).

Low frequency measurements. Electromagnetic properties in low-frequency range (1 kHz-2 MHz) were investigated using an impedance meter LCR Agilent E4980A. The 1.9 mm thick flat samples were placed in the space between capacitor plates and their complex impedance was measured. The obtained experimental data was then used to calculate the complex dielectric permittivity of the sample under study.

Microwave measurements in Ka-band (26-37 GHz). The microwave measurements were carried out in a 7.2x3.4 waveguide transmission line using a scalar network analyzer ELMIKA R2-408R. In a typical experiment, the flat sample was placed in the closed waveguide system normal to the incident radiation wavevector. The amplitudes of reflected (S_{11}) and transmitted (S_{21}) signals were then measured within 26-37 GHz (Ka-band) frequency range. The measurements procedure is described in detail in our previous work [18]. The dielectric permittivity ε was then calculated based on the methodology described in [19].

Terahertz measurements. The terahertz measurements were performed using a commercial THz time-domain spectrometer 'Tspec' by EKSPLA. The detailed description of the experimental setup was described in [20]. The measurements of the complex transmission coefficient of a plane wave normally scattered on flat samples in the free space were performed in the frequency range 0.2-1.0 THz. The upper-frequency limit was defined by the low transparency of investigated CR samples for terahertz radiation. The dielectric permittivity ε was then calculated based on the methodology similar to the microwave range described in [19].

Table 1. Specifications of the chloroprene rubber composition

Test description		Indicator	Method	ASTM D2000 requirement
	Metric system	M		
	Chloroprene rubber	3BE		
Neat CR	Tensile Strength, min, MPa	614	ASTM D412	14
	Elongation, min, %	614	ASTM D412	350
	Hardness	614	ASTM D2240	60±5
	Tear resistance, Die C, min, kN/m	G21	ASTM D624	26
Heat resistance 70 hr at 100°C	Tensile Strength Change, max, MPa	A14	ASTM D573	-15
	Change of Elongation, max, %	A14	ASTM D573	-40
	Change of Hardness, max Shore A	A14	ASTM D573	+15
Compression set, 22 hr at 100°C, max, %		B14	ASTM D 395(B)	25
Immersion in IRM 901, 70 hr at 100°C	Change of Tensile Strength, MPa	EO14	ASTM D471	-30
	Change of Elongation, %	EO14	ASTM D 471	-30
	Change of Hardness, max Shore A	EO14	ASTM D471	±10
	Change in volume %	EO14	ASTM D471	-10 to +15
Adhesion strength rubber/metal ,min, MPa		K11	ASTM D 429 (A)	1.4
Low temperature resistance, nonbrittle after 3 min at -55°C		F19	ASTM D2137 (C)	Pass
Ozone resistance, quality retention rating, min, %		C12	ASTM D1171	100
LOI index, min,%		Z1	ASTM D2863	35

Table 2. Mechanical properties of chloroprene rubber materials

Sample	Tensile Strength, MPa	Elongation to Break, %	Hardness (Shore A)
A) Neat CR	13.3	289	57
B) UV ageing	12.3	271	67
C) Immersion	5.7	205	-
D) Thermal	13.0	260	64
E) Thermal+ +Immersion	1.8	188	24

3. Experimental results

The properties of the CR (neat and aged) were tested and found to comply with ASTM D2000: M3BE 614 A14 B14 C12 EO14 F19 G21 K11 Z1, as shown in Table 1. Mechanical properties after ageing are shown in Table 2.

Analysis of Table 2 shows, that the tensile strength decreases after all types of degradation processes. The largest change was observed for CR samples thermally aged in combination with oil immersion. For these samples, E-series, the hardness decreases by roughly 50% and the strength falls by 85%. The combination of heat and oil is catastrophic to this kind of rubber. **Thermally aged and UV aged** samples show an increase in hardness after degradation. According to [21] the increase of hardness is typically related to the crosslinking mechanisms in the polymer chain. On the other

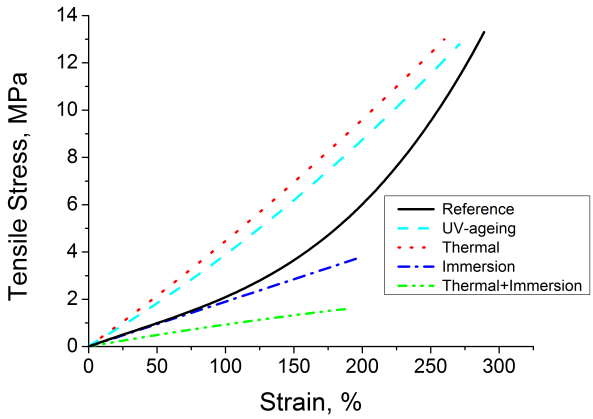

Figure 1. Typical stress-strain curves of rubber specimens.

hand, the decrease of hardness is usually associated to either swelling with concomitant softening by oil (physical ageing mechanism), and/or chain scission (chemical ageing mechanism). **Stress-strain curves in Fig. 1 demonstrate the effect of ageing on properties. UV exposure (B-series) leads to an increase in modulus, correlative with the increase in hardness, whereas oil immersion results in a decrease in modulus. Nevertheless, the combined effect of thermal ageing and oil immersion (E-series) leads to a significant reduction in both strength and the elongation to break, due to chain scission and the inability of the shorter chains to withstand stretch. Shorter-term oil immersion (C-series) shows a more moderate decrease in modulus, however, the elongation is strongly affected similarly to the long-term exposure. In a way, oil immersion prevents thermal oxidation, and accelerated ageing in oil at 100°C mostly reflects the accelerated oil absorption resulting in modulus decrease with a similar elongation to break when compared to short-term oil immersion. Strain hardening is also prevented in oil. Short-term thermal ageing (D-series) has a similar effect to UV exposure, leading to further crosslinking and modulus increase.**

The results of the calculation of the dielectric permittivity from the experimentally measured data in the low frequency, microwave-, and THz ranges are presented in Fig.2 (a), (b), (c), correspondingly. First, form Fig.2 a good correspondence is obserwed between different types of constituent parameters reconstruction in different frequency ranges: capacitor impedance measurements at low frequencies, the waveguide in the microwave and free space in THz range. The general and universal result for all frequency ranges may be concluded as follows. From Fig.2 it is clearly seen that thermal degradation together with the immersion of oil leads to a decrease of both real and imaginary parts of dielectric permittivity within all frequency regions. Ultraviolet and thermal ageing without immersion lead vice-versa to an increase of the dielectric

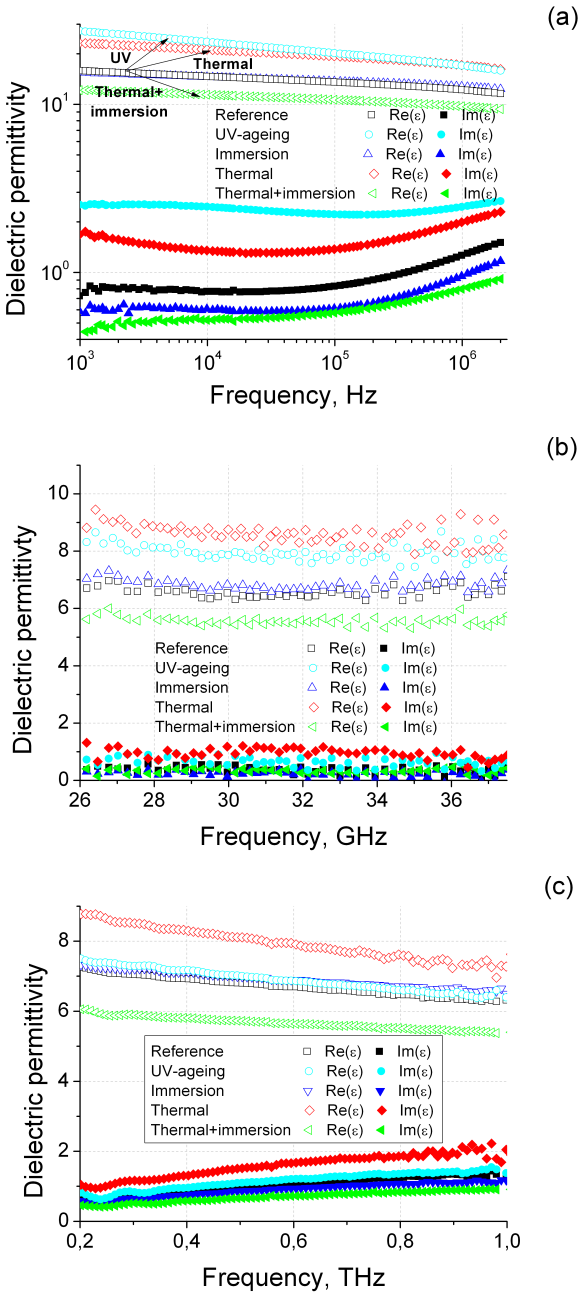

Figure 2. Frequency dependence of dielectric permittivity ε of CR materials in low frequency (a) in the Ka-band (b) and in terahertz range (c).

permittivity of the samples under study. The UV-ageing has the largest impact on dielectric permittivity of CR samples at low frequencies, and thermal degradation - in microwave and terahertz ranges. The immersion at normal conditions affects minorly the dielectric permittivity spectra, especially at high frequencies. A more detailed examination for each frequency range follows.

The quasistatic values of dielectric permittivity of unaged CR are in good

correlation with [2, 3]. From low-frequency spectra in Fig.2 (a) we can see that the real part of dielectric permittivity is decreasing with frequency. The imaginary part of ε generally increases. This is typical quasi-Debye behavior typical for polymers in the low frequency range. Particularly, the reduction of the real part of dielectric permittivity with frequency is directly related to the Debye relaxation caused by delay for the orientation of the dipoles in the high frequency oscillating electric field [22, 23].

Important to note that the maximum of $Im(\varepsilon)$ observed in carbon black/CR composites [2] near 1 MHz is typical for carbon-containing polymer materials [23]. This maximum was not observed in the neat and degraded CR at room temperature in the present study. The detailed inspection of Fig.1 (a) shows that the $Im(\varepsilon)$ curves are low-grade S-shaped. The possible origin of this behavior may be a combination of different relaxation processes mentioned in [2] which are significantly blurred and damped at the room temperature.

The observed decrease in dielectric permittivity after thermal degradation combined with oil immersion is most probably related to the volume change of the material. Samples exposed to thermal degradation and oil immersion after 35 days at 100°C were shown to swell significantly, with a volume increase of 71%, thus leading to a decrease in the number of highly polarized C-Cl bonds per unit volume. Extraction of the chlorinated plasticizer during exposure to oil is also expected, thus further decreasing the concentration of C-Cl bonds [2, 3]. Dehydrochlorination by chain scission is another viable ageing mechanism.

Thermal degradation and UV ageing without immersion lead to an increase of dielectric permittivity within all investigated frequency ranges. It is well known that the polymers can be deteriorated by UV radiation and some polar groups such as carboxyl and hydroxyl are formed in the polymer after thermal and UV exposure [24]. In this case, the effective dielectric permittivity will increase. From Fig.2 (a) we can see that at low frequencies the UV-ageing has the largest impact on dielectric permittivity. Meanwhile, the permittivity of UV-aged samples is decreasing with frequency most intensively in comparison to other samples. Above 1 MHz the $Re(\varepsilon)$ of UV- and thermally-aged samples becomes comparable.

The inspection of Fig.2 (b) shows that samples under study have almost constant dielectric permittivity in 26-37 GHz range. This is in good correlation with many previous studies of dielectric materials [25] which are typically weak dispersive in this relatively narrow frequency range. Nevertheless, it is shown below in the next section that this microwave region may be effectively used for quick detection of degradation in CR-based materials. Likewise in the low-frequency region the thermal degradation and the UV ageing without immersion lead to an increase of ε, but in microwave range the thermal-ageing has the largest impact on dielectric permittivity.

The general frequency dependencies of ε observed in low frequency and in microwave ranges also continue in the terahertz region (Fig.2 (c)). Important to note, the growth of $Im[\varepsilon]$ at such high frequencies makes the CR material very lossy and opaque for electromagnetic waves. In this region the UV-ageing as well as oil immersion lead to

minor increases of dielectric permittivity. The thermally aged samples without and with oil immersion have increased and decreased dielectric permittivity in the terahertz range, correspondingly.

4. Express method to detect degradation

The EM investigations described above require special precise sample preparation for measurements. We will show in this section that specific features of microwave radiation and physical properties of CR may be effectively combined in non-invasive degradation detection method which may prove very useful in large CR-surfaces inspection. From Fig.2 one can see that CR materials have relatively high values of dielectric permittivity (about 6-9) at relatively small (compared to radio frequency) wavelength (1 cm for 30 GHz). Additionally, CR is semi-transparent for microwaves - this fact allows to organize precise measurements for mm-sized samples, most commonly used in the practice.

If the optical length of the sample in the specific frequency range is equal to the half wavelength of microwave radiation, the minimum of reflection is observed in case of normal plane wave scattering. We propose to utilize this interference minimum peak for detection of material degradation. This EM express test seems to be competitive with other characterization methods because now the cheap and compact microwave reflectometers are available on the market [26] especially at low GHz frequencies. Moreover, the similar principle was already evaluated in [27] for fuel level detection in tanks. To demonstrate quick measurements method we will use Ka-band but the results below are also valid for other commonly used frequency ranges (X-band, Ku-band etc.). In case of waveguide measurements it is possible to calculate amplitudes of reflected S_{11} and transmitted S_{21} through the sample signals using the following relationships based on Fresnel formulas [28] (equations are given in SI units, assuming an $\exp[i(kz-\omega t)]$ dependence of the incident electric field):

$$S_{11} = \frac{-\sin(\gamma\tau)\left(\gamma_0^2-\gamma^2\right)}{\sin(\gamma\tau)\left(\gamma^2+\gamma_0^2\right)+2i\gamma\gamma_0\cos(\gamma\tau)}; \tag{1}$$

$$S_{21} = \frac{2\gamma/\gamma_0}{-2\gamma/\gamma_0\cos(\gamma\tau)+i\left((\gamma/\gamma_0)^2+1\right)\sin(\gamma\tau)}, \tag{2}$$

where $\gamma = \sqrt{\left(\frac{2\pi}{\lambda}\right)^2\varepsilon-\left(\frac{\pi}{a}\right)^2}$, $\gamma_0 = \sqrt{\left(\frac{2\pi}{\lambda}\right)^2-\left(\frac{\pi}{a}\right)^2}$, τ is the sample's thickness, $a = 7.2$ mm is the width of the waveguide, $\lambda = c/\nu$ the wavelength, c the vacuum light velocity, ν is the frequency and ε is the complex dielectric permittivity of the investigated sample.

Inspection of Eq.(1)-(2) shows that the frequency position of reflection minimum peak is dependent on layer thickness and its complex dielectric permittivity. To demonstrate them in Fig.3 are presented S-parameters (amplitude of reflected S_{11} and transmitted S_{21} signal) of 1.9 mm thick layer of CR rubber in the waveguide (closed symbols), along with results of modelling (in the form of lines) based on Eq.(1)-(2) with $\varepsilon = 6.8 + i0.35$.

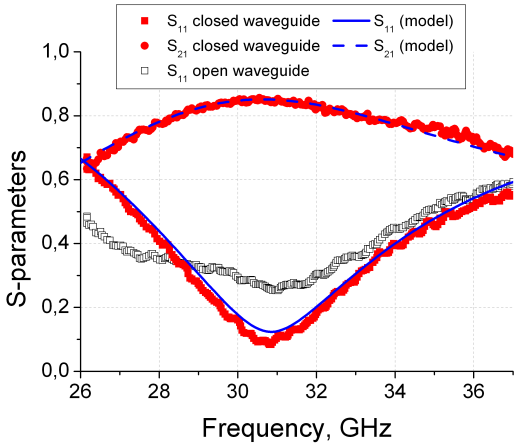

Figure 3. Experimental S-parameters of 1.9 mm thick layer of CR rubber in the waveguide (closed symbols), results of modeling (lines) and the S_{11} spectra of open waveguide flange covered by 1.9 mm thick layer of CR rubber (open symbols).

It is interesting to note that in order to observe the minimum reflection in thin samples (1-2 mm), it is not necessary to cut and place them in the closed waveguide. It is sufficient to simply lean the material on the open flange of the waveguide.

The open waveguide flange covered with a layer of the investigated material is, of course, a complicated open system. For precise calculation of such a system the effects such as reflection of radiation from the open edge of the waveguide, radiation in the free space etc. should be taken into account. Nevertheless, in the case when the thickness of the layer is small (several millimeters) in comparison to wavelength, the reflection minimum is observable. Moreover, the reflection peak is located at the same frequency as in the conventional closed waveguide measurements. The S_{11} spectra of open waveguide flange covered by 1.9 mm thick layer of CR rubber is presented in Fig.3 by open symbols. We see from this figure that the peak in the open flange measurements is not so sharp in comparison to the closed waveguide. This is because of partial radiation of scattered wave into the free space. But the position of interference peak is still the same. A similar tendency was observed also for other investigated samples. This fact allows **to use S_{11} spectra with a sharp reflection minimum for** testing of large surfaces of CR without special preparation for measurements. When the interference peak of an unaged piece of CR is detected and identified, the investigated large surface may be then scanned by the simple moving of the waveguide flange above them. In many practical cases, the thickness of CR is constant in the investigated surface and the change of reflection peak position may be correlated to degradation of the material near current waveguide flange position.

Results of typical open flange S_{11} measurements for three investigated samples are presented in Fig.4 with symbols. The maximum positions are in good correspondence with expected values (see modeling results presented by lines). We point out again that just by applying the open waveguide flange on the investigated CR surface, then shifting

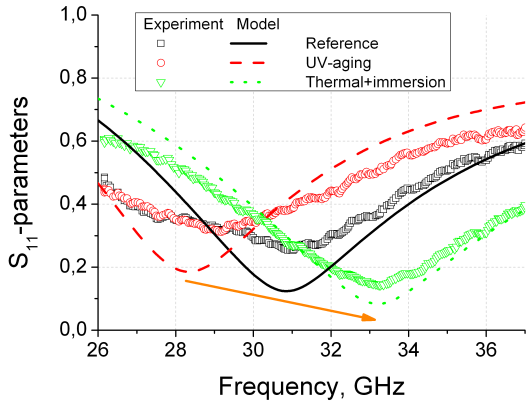

Figure 4. Experimental S_{11}-parameters of open waveguide flange covered by 1.9 mm thick layer of the CR-based samples (symbols), results of modeling (lines), the arrow shows the direction of decrease of ε.

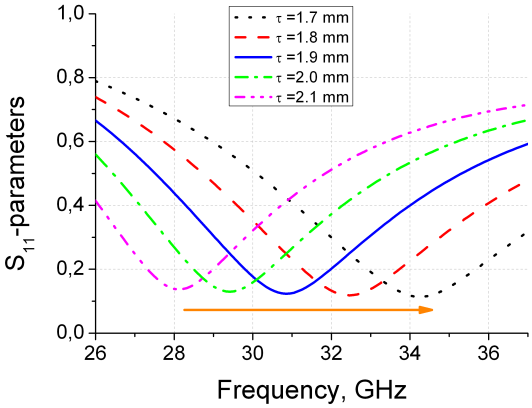

Figure 5. Calculated S-parameters of CR rubber ($\varepsilon = 7 + i0.38$) in the waveguide with various layer thickness τ, the arrow shows the direction of decrease of τ from 2.1 to 1.7 mm.

to next area, it is possible to analyze and detect degraded areas fast in a non-destructive way.

In practice, the thickness of the investigated surface may be not constant and have some fluctuations. In this case, it is very important to know how to distinguish the effects of thickness irregularity and dielectric permittivity change.

From Fig.4 we see that the change of electromagnetic properties of samples with equal thicknesses leads to both shift of peak position and change in their amplitude. The basic analysis of Eq.(1) for S_{11} shows that the effect of thickness irregularity (within 10%) will also affect the peak position but its absolute value of amplitude will change in a minor fashion in comparison to free space radiation losses. This effect is clearly seen in Fig. 5.

Summarising, if by using an open flange measurement procedure as described above a) the reflection minimum is shifted and b) its amplitude changes in comparison to the reference material, so this is an evidence of a significant change of the dielectric permittivity in the investigated spot, which in the case of CR-based materials is related to degradation. In case of thermal degradation the peak shifts to the right and in case of UV ageing - to the left in the high- low-frequency region, correspondingly.

5. Discussion and Conclusions

The wide range of CR-based materials applications require effective, compact and mobile tools suitable for non-destructive diagnostic of such systems. The measurement of ε in the frequency-domain may offer important and useful information about material degradation.

The results presented in this broadband dielectric spectroscopy investigation show a well-defined correlation between degradation of CR and the change of its dielectric permittivity. The most probable mechanisms of degradation are swelling and extraction of plasticizer in the case of immersion in oil, coupled with chemical mechanisms such as dehydrochlorination reactions and forming of polar carboxyl and hydroxyl groups in the polymer matrix in the case of thermal ageing. Within the frequency range 1 kHz - 1.0 THz we observed that the thermal degradation together with the immersion of oil leads to a decrease of both real and imaginary parts of dielectric permittivity. Ultraviolet and thermal ageing without immersion led vice-versa to an increase of the dielectric permittivity of the samples under study. The relative change of dielectric permittivity of aged and unaged samples (> 10 %) was enough to use an open flange method to perform non-destructive testing of CR samples, and this result implies that CR rubber parts with large surface areas subjected to ageing conditions could be analyzed by this express detection method of degraded regions.

Acknowledgments

The work is supported by H2020 RISE 734164 Graphene 3D and COST Action CA15107 MultiComp. DB and PK are thankful for support by Tomsk State University Competitiveness Improvement Program. **PK is thankful to the Grant of the President of the Republic of Belarus in science, education, health, and culture in 2019. RS and NN are grateful to Gumian Ltd. for the rubber compound.**

References

[1] Deepalekshmi Ponnamma, Kishor Kumar Sadasivuni, Chaoying Wan, Sabu Thomas, and Mariam Al-Ali AlMa'adeed. *Flexible and stretchable electronic composites*. Springer, 2015.

[2] H Kuwahara, S Sudo, M Iijima, and S Ohya. Dielectric properties of thermally degraded chloroprene rubber. *Polymer Degradation and Stability*, 95(12):2461–2466, 2010.

[3] A Das, AK Ghosh, and DK Basu. Evaluation of physical and electrical properties of chloroprene rubber and natural rubber blends. *KGK-Kautschuk Gummi Kunststoffe*, 58(5):230–238, 2005.

[4] HL Stephens. Textbook for intermediate correspondence course, 1985.

[5] Siti Zuliana Salleh, Hanafi Ismail, and Zulkifli Ahmad. The effect of pre-and post-electron beam irradiation on the properties of nr/rcr blends. In *AIP Conference Proceedings*, volume 1865, pages 040020–. AIP Publishing, 2017.

[6] A Saritha Chandran and Sunil K Narayanankutty. An elastomeric conducting composite based on polyaniline coated nylon fiber and chloroprene rubber. *European Polymer Journal*, 44(7):2418–2429, 2008.

[7] L Olmedo, G Chateau, C Deleuze, and JL Forveille. Microwave characterization and modelization of magnetic granular materials. *Journal of applied physics*, 73(10):6992–6994, 1993.

[8] Chi-Hau Chen. *Ultrasonic and advanced methods for nondestructive testing and material characterization*. World Scientific, 2007.

[9] Revathy Ravindren, Subhadip Mondal, Poushali Bhawal, Shek. Mahammad Nasim Ali, and Narayan Chandra Das. Superior electromagnetic interference shielding effectiveness and low percolation threshold through the preferential distribution of carbon black in the highly flexible polymer blend composites. *Polym. Compos.*, 0(0), March 2019.

[10] Revathy Ravindren, Subhadip Mondal, Krishnendu Nath, and Narayan Ch Das. Investigation of electrical conductivity and electromagnetic interference shielding effectiveness of preferentially distributed conductive filler in highly flexible polymer blends nanocomposites. *Composites Part A: Applied Science and Manufacturing*, 118:75–89, 2019.

[11] Subhadip Mondal, Lalatendu Nayak, Mostafizur Rahaman, Ali Aldalbahi, Tapan K. Chaki, Dipak Khastgir, and Narayan Ch Das. An effective strategy to enhance mechanical, electrical, and electromagnetic shielding effectiveness of chlorinated polyethylene-carbon nanofiber nanocomposites. *Composites Part B: Engineering*, 109:155–169, 2017.

[12] Revathy Ravindren, Subhadip Mondal, Krishnendu Nath, and Narayan Ch Das. Prediction of electrical conductivity, double percolation limit and electromagnetic interference shielding effectiveness of copper nanowire filled flexible polymer blend nanocomposites. *Composites Part B: Engineering*, 164:559–569, May 2019.

[13] Subhadip Mondal, Sabyasachi Ghosh, Sayan Ganguly, Poushali Das, Revathy Ravindren, Subhashis Sit, Goutam Chakraborty, and Narayan Ch Das. Highly conductive and flexible nano-structured carbon-based polymer nanocomposites with improved electromagnetic-interference-shielding performance. *Materials Research Express*, 4(10):105039, October 2017.

[14] Subhadip Mondal, Sayan Ganguly, Poushali Das, Dipak Khastgir, and Narayan Ch Das. Low percolation threshold and electromagnetic shielding effectiveness of nano-structured carbon based ethylene methyl acrylate nanocomposites. *Composites Part B: Engineering*, 119:41–56, June 2017.

[15] Subhadip Mondal, Sayan Ganguly, Mostafizur Rahaman, Ali Aldalbahi, Tapan K. Chaki, Dipak Khastgir, and Narayan Ch. Das. A strategy to achieve enhanced electromagnetic interference shielding at low concentration with a new generation of conductive carbon black in a chlorinated polyethylene elastomeric matrix. *Phys. Chem. Chem. Phys.*, 18(35):24591–24599, 2016.

[16] Subhadip Mondal, Poushali Das, Sayan Ganguly, Revathy Ravindren, Sanjay Remanan, Poushali Bhawal, Tushar Kanti Das, and Narayan Ch. Das. Thermal-air ageing treatment on mechanical, electrical, and electromagnetic interference shielding properties of lightweight carbon nanotube based polymer nanocomposites. *Composites Part A: Applied Science and Manufacturing*, 107:447–460, April 2018.

[17] Rubber compound 70-075-12, gumian ltd., lod, israel.

[18] D. Bychanok, G. Gorokhov, D. Meisak, A. Plyushch, P. Kuzhir, A. Sokal, K. Lapko, A. Sanchez-Sanchez, V. Fierro, A. Celzard, C. Gallagher, A. P. Hibbins, F. Y. Ogrin, and C. Brosseau. Exploring carbon nanotubes/batio3/fe3o4 nanocomposites as microwave absorbers. *Progress In Electromagnetics Research C*, 66:77–85, 2016.

[19] Standard test method for measuring relative complex permittivity and relative magnetic permeability of solid materials at microwave frequencies, astm d5568-08, 2009.

[20] D. Bychanok, P. Angelova, A. Paddubskaya, D. Meisak, L. Shashkova, M. Demidenko, A. Plyushch, E. Ivanov, R. Krastev, R. Kotsilkova, F. Y. Ogrin, and P. Kuzhir. Terahertz absorption in graphite nanoplatelets/polylactic acid composites. *Journal of Physics D: Applied Physics*, 51(14):145307, 2018.

[21] James E Mark, Burak Erman, and Mike Roland. *The science and technology of rubber*. Academic press, 2013.

[22] Andrew K Jonscher. Dielectric relaxation in solids. *Journal of Physics D: Applied Physics*, 32(14):R57–, 1999.

[23] D Bychanok, P Kuzhir, S Maksimenko, S Bellucci, and Christian Brosseau. Characterizing epoxy composites filled with carbonaceous nanoparticles from dc to microwave. *Journal of Applied Physics*, 113(12):124103–, 2013.

[24] M Ehsani, H Borsi, E Gockenbach, J Morshedian, GR Bakhshandeh, and AA Shayegani. Effect of aging on dielectric behavior of outdoor polymeric insulators. In *Solid Dielectrics, 2004. ICSD 2004. Proceedings of the 2004 IEEE International Conference on*, volume 1, pages 312–315. IEEE, 2004.

[25] Bill Riddle, James Baker-Jarvis, and Jerzy Krupka. Complex permittivity measurements of common plastics over variable temperatures. *IEEE Transactions on Microwave theory and techniques*, 51(3):727–733, 2003.

[26] www.planarchel.ru.

[27] Kaida Khalid, Ionel Valeriu Grozescu, Lim Keng Tiong, Lee Teck Sim, and Roslim Mohd. Water detection in fuel tanks using the microwave reflection technique. *Measurement Science and Technology*, 14(11):1905–, 2003.

[28] D Bychanok, A Plyushch, K Piasotski, A Paddubskaya, S Voronovich, P Kuzhir, S Baturkin, A Klochkov, E Korovin, and Maxime Letellier. Electromagnetic properties of polyurethane template-based carbon foams in ka-band. *Physica Scripta*, 90(9):094019–, 2015.